Electronic Supplementary Material (ESI) for Dalton Transactions.

Supplementary information for

Insights from partially oriented CW-EPR spectroscopy studies into the interaction of lytic polysaccharide monooxygenases with cellulose

Luisa Ciano, Alessandro Paradisi, Glyn R. Hemsworth, Morten Tovborg, Gideon J. Davies and Paul H. Walton*

Supplementary figures, tables and appendix

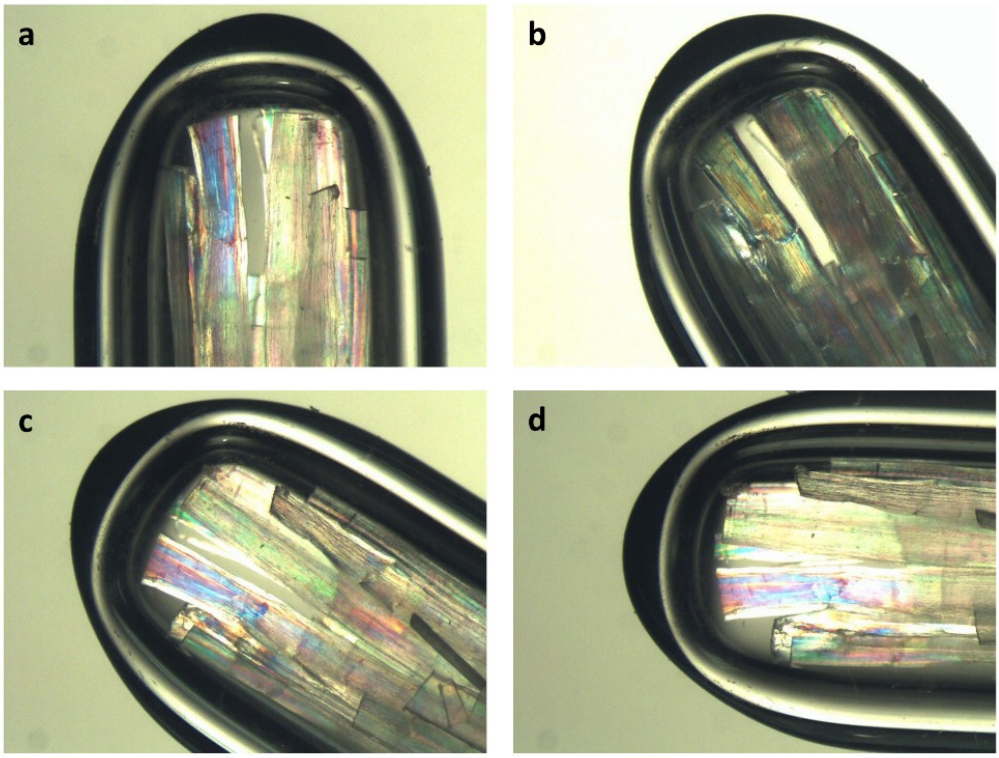

Fig. S1 Celery cellulose fibres under polarised light. (a) Starting position; (b) 30° rotation, (c) 60° rotation, (d) 90° rotation.

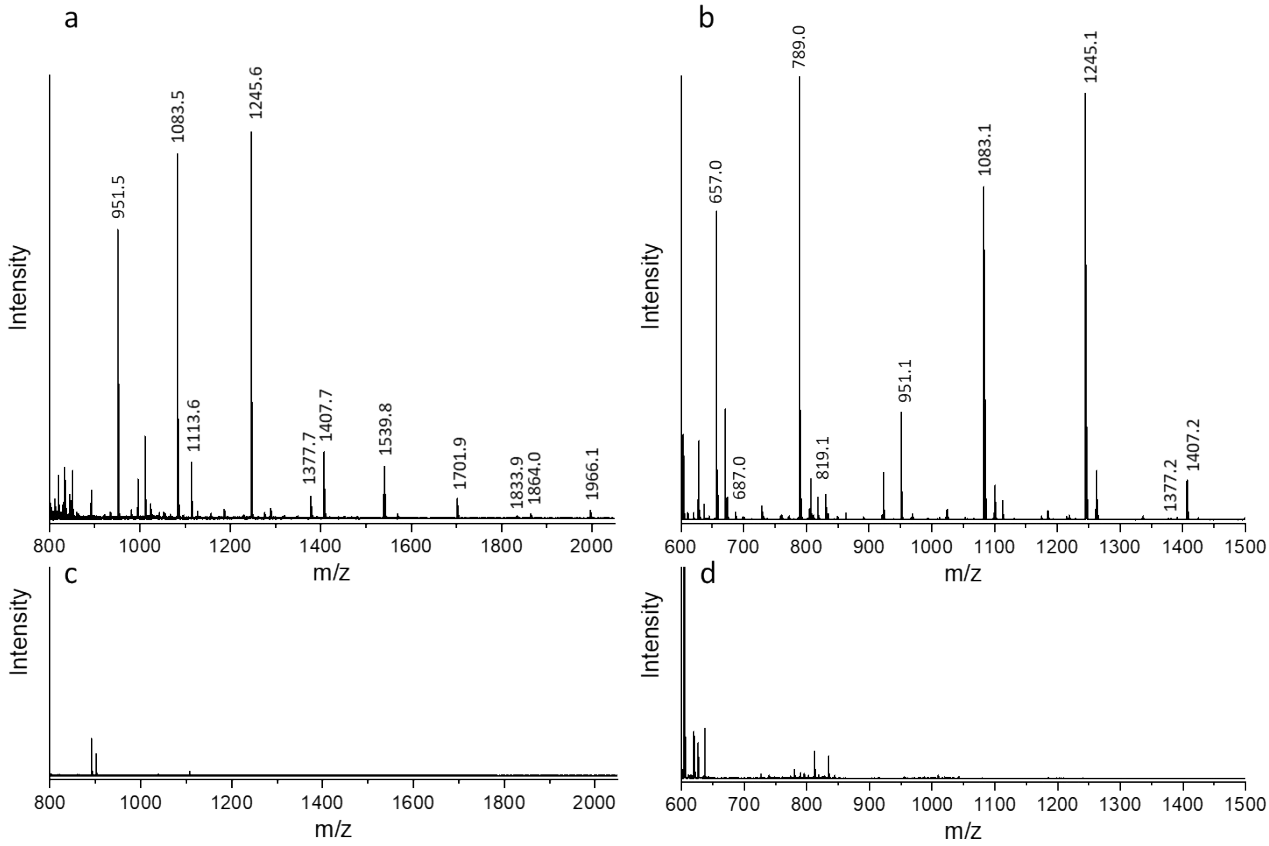

Fig. S2 MALDI-TOF mass spectra of soluble enzymatic oligosaccharide products following incubation of *Ta*AA9A (a) or *Ls*AA9A (b) with celery fibres and ascorbic acid; (c) and (d) show respective control reactions conducted in the absence of ascorbic acid.

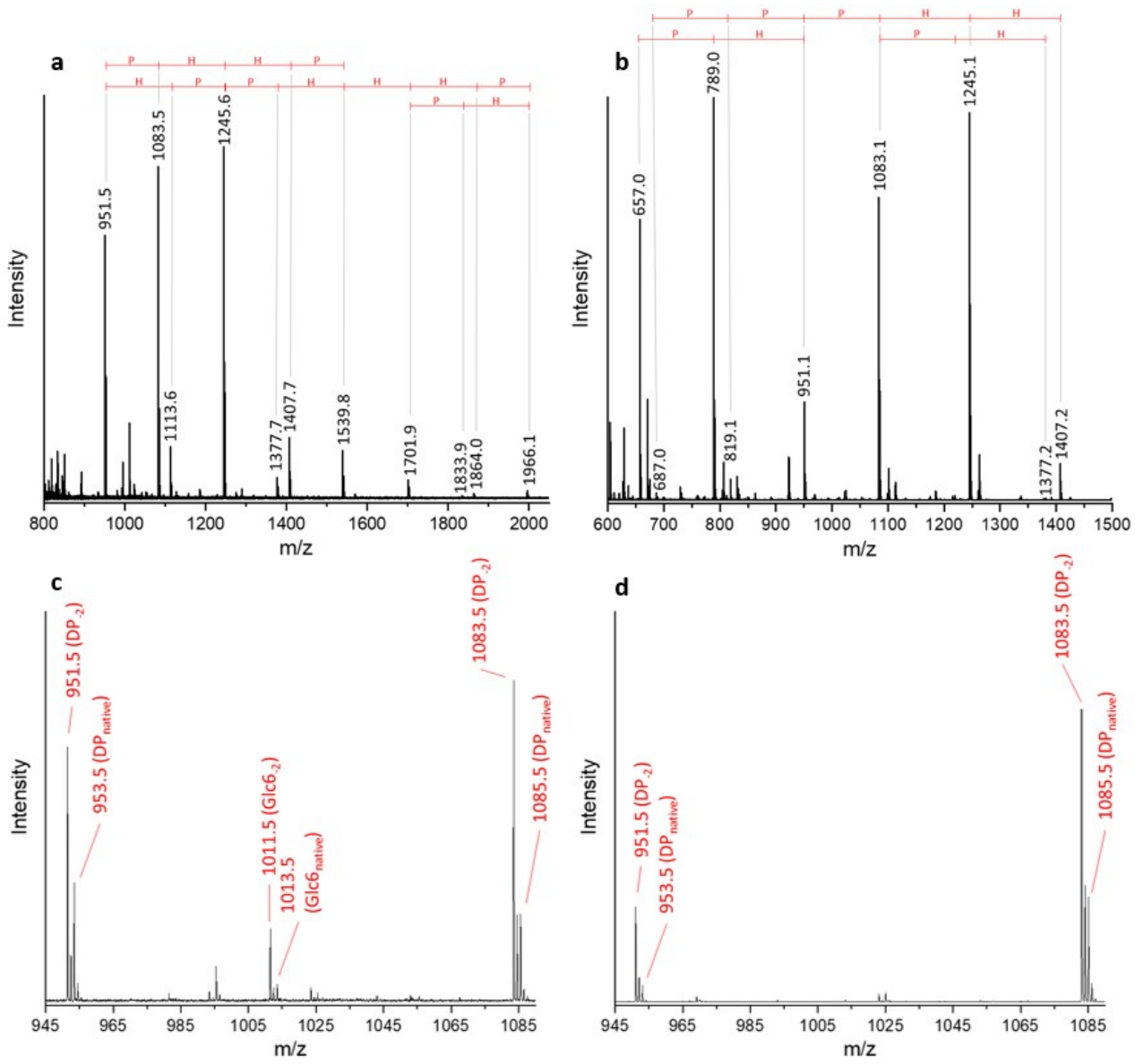

Fig. S3 MALDI-TOF mass spectra of soluble products of incubation of *Ta*AA9A (a) or *Ls*AA9A (b) with celery fibres with and ascorbate. The H and P labels correspond to a mass difference of 162 Da (hexose unit) or 132 Da (pentose unit), respectively. Figures (c) and (d) are zoomed-is views respect to spectra (a) and (b), respectively, showing the non-oxidized mixed chain (DP_{native}) together with the corresponding C4 oxidized analog (DP_{-2}). Glc_{native} and Glc_{-2} refer to native cellohexaose and C4 oxidized cellohexaose, respectively. All species reported correspond to the monosodiated adducts ($+Na^+$).

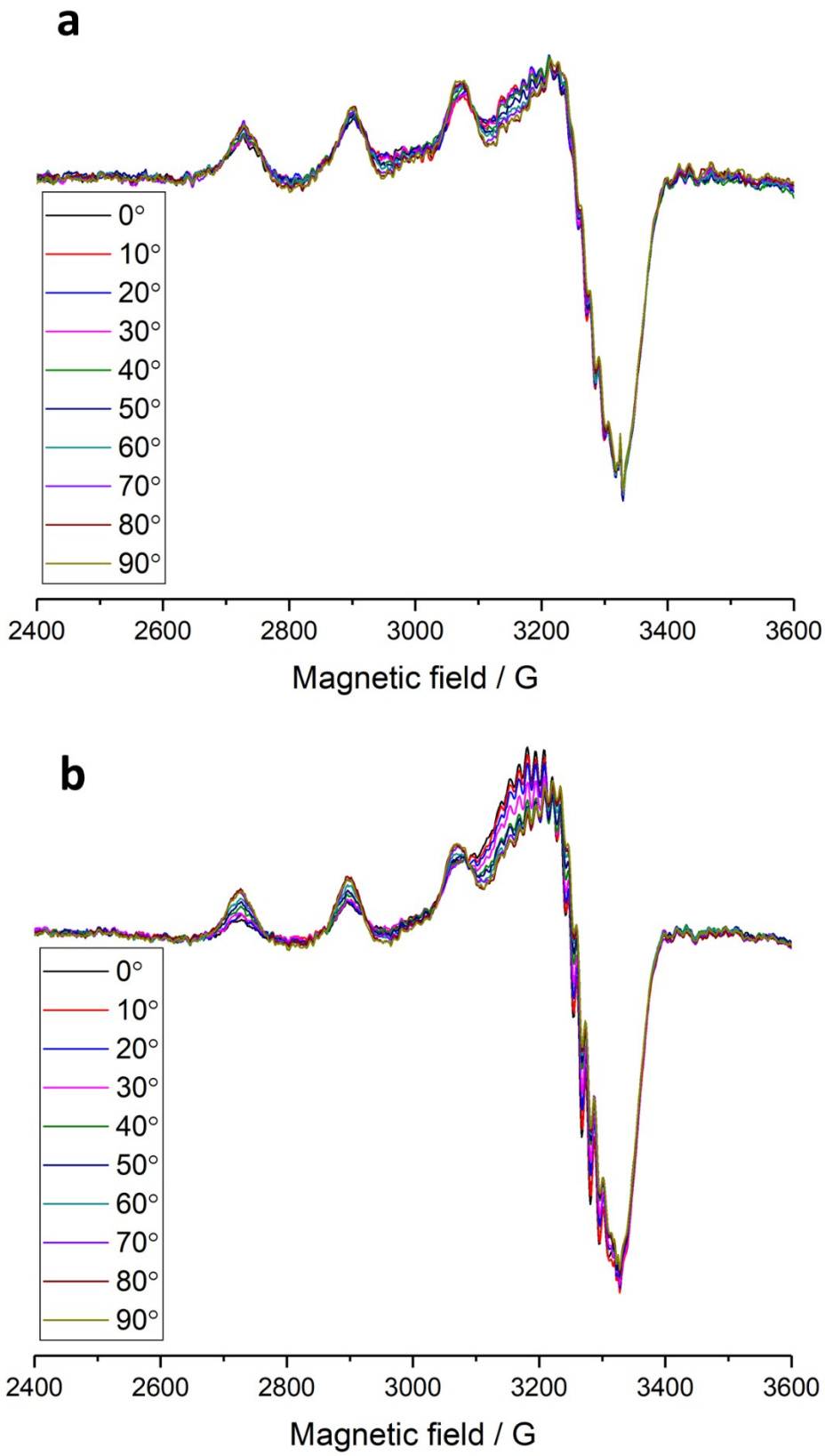

Fig. S4 CW EPR spectra of *Ls*AA9A on celery fibres. (a) fibres arranged as in Fig. 2b. (b) Fibres arranged as in Fig. 2c.

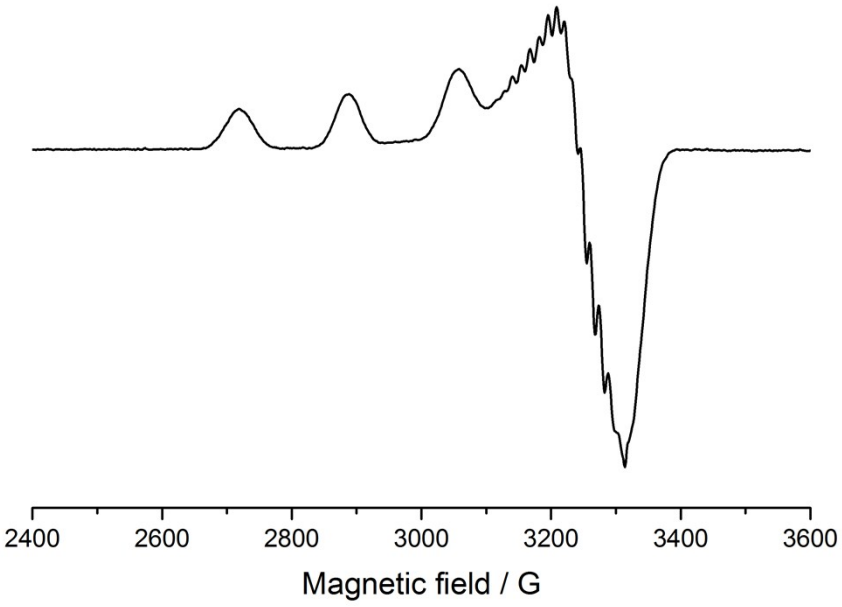

Fig. S5 CW EPR spectrum of *Ls*AA9A in the presence of excess cellohexaose and NaCl.

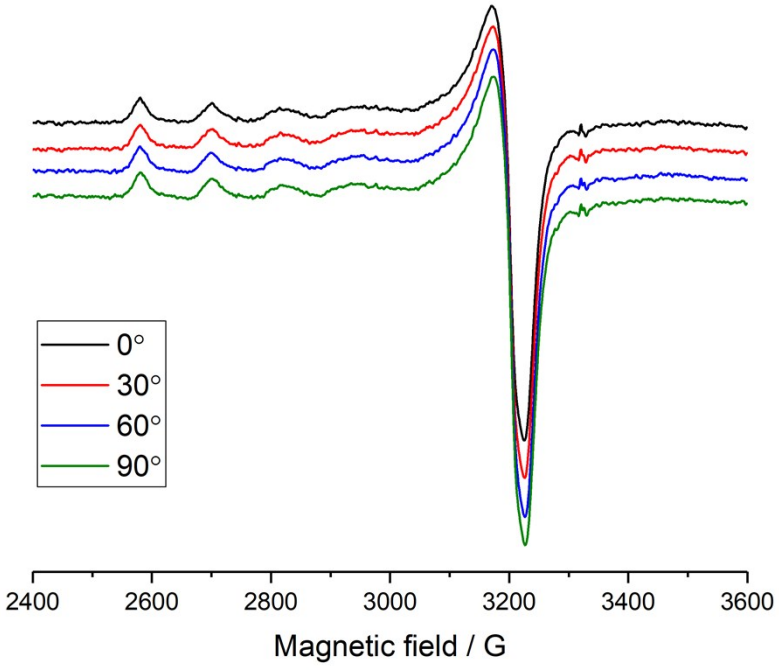

Fig. S6 CW EPR spectra of a 5 mM $CuCl_2$ solution collected at different orientations with respect to the static magnetic field using the cell described in Fig. 2a.

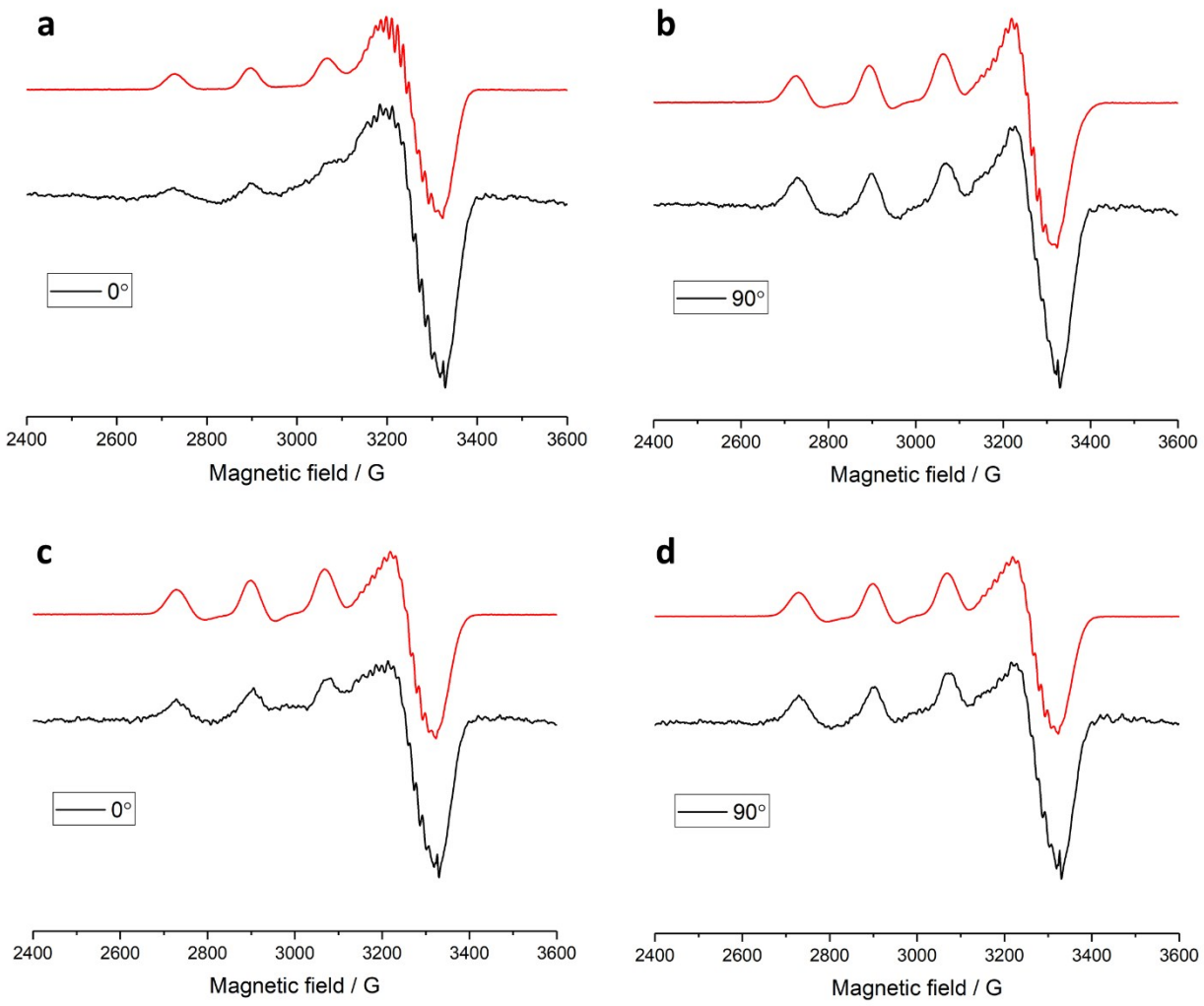

Fig. S7 Simulations (red) and experimental data (black) for EPR spectra of *Ls*AA9A on celery collected using the fibres arrangement in Fig. 2a (a and b) or Fig. 2b (c and d). The simulations clearly reproduce the trends of the experimental data and were obtained in all cases using the values reported in Table 1. For clarity, only these two angles are shown. Full 0°-180° rotation for the Fig. 2a fibres arrangement is shown in Movie S3.

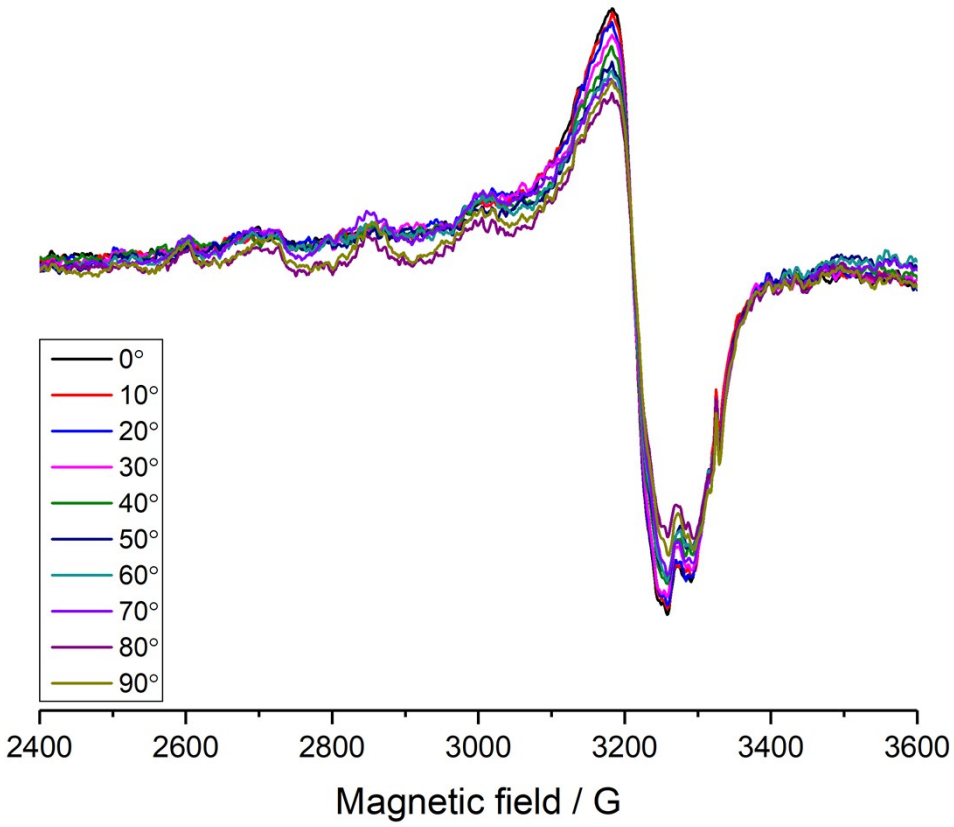

Fig. S8 EPR spectra of *Ta*AA9A on celery fibres in the arrangement shown in Fig. 2a, collected between 0° and 90° with respect to the static magnetic field, where 0° represent the position with the long axis of the fibres parallel to $\vec{B}_0$.

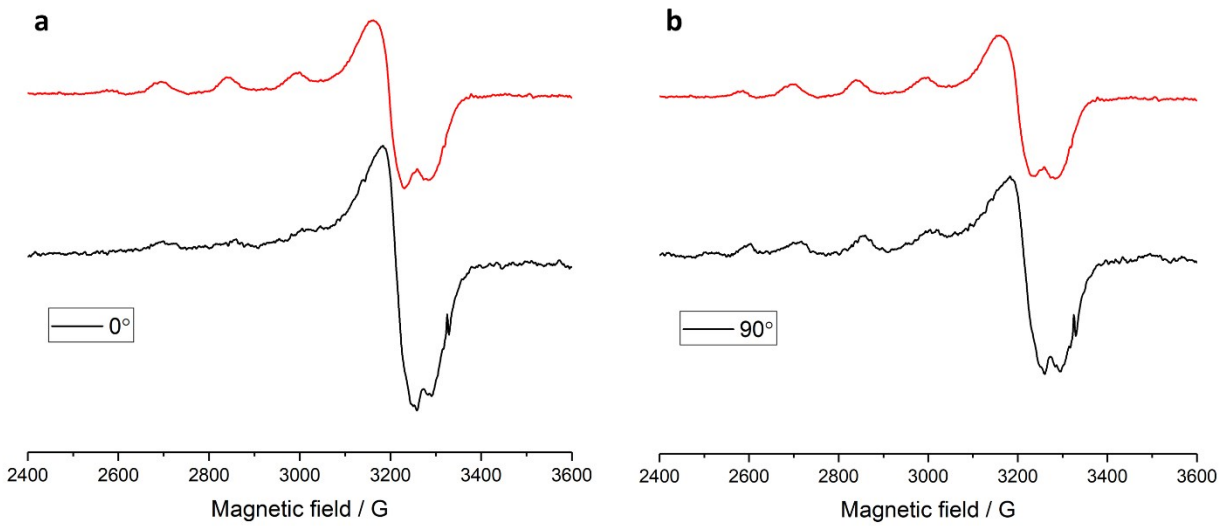

Fig. S9 Simulations (red) and experimental data (black) for EPR spectra of *Ta*AA9A on celery collected using the fibre arrangement in Fig. 2a. The simulations reproduce the trends of the experimental data and were obtained using the values reported in Table 1.

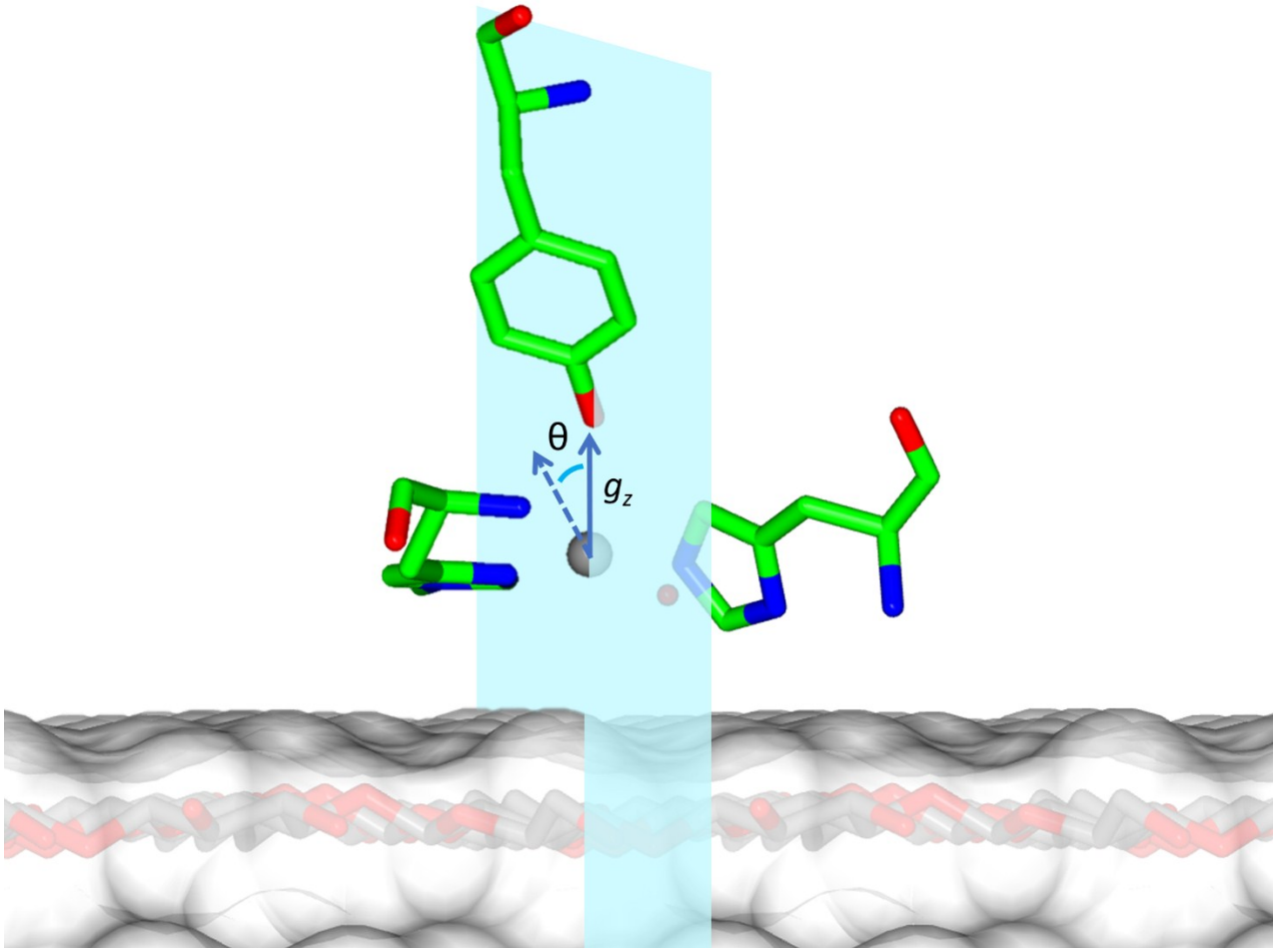

Fig. S10 Scheme illustrating the relationship between the orientation of the g_z axis with respect to the flat surface of the cellulose fibres that defines the angle θ.

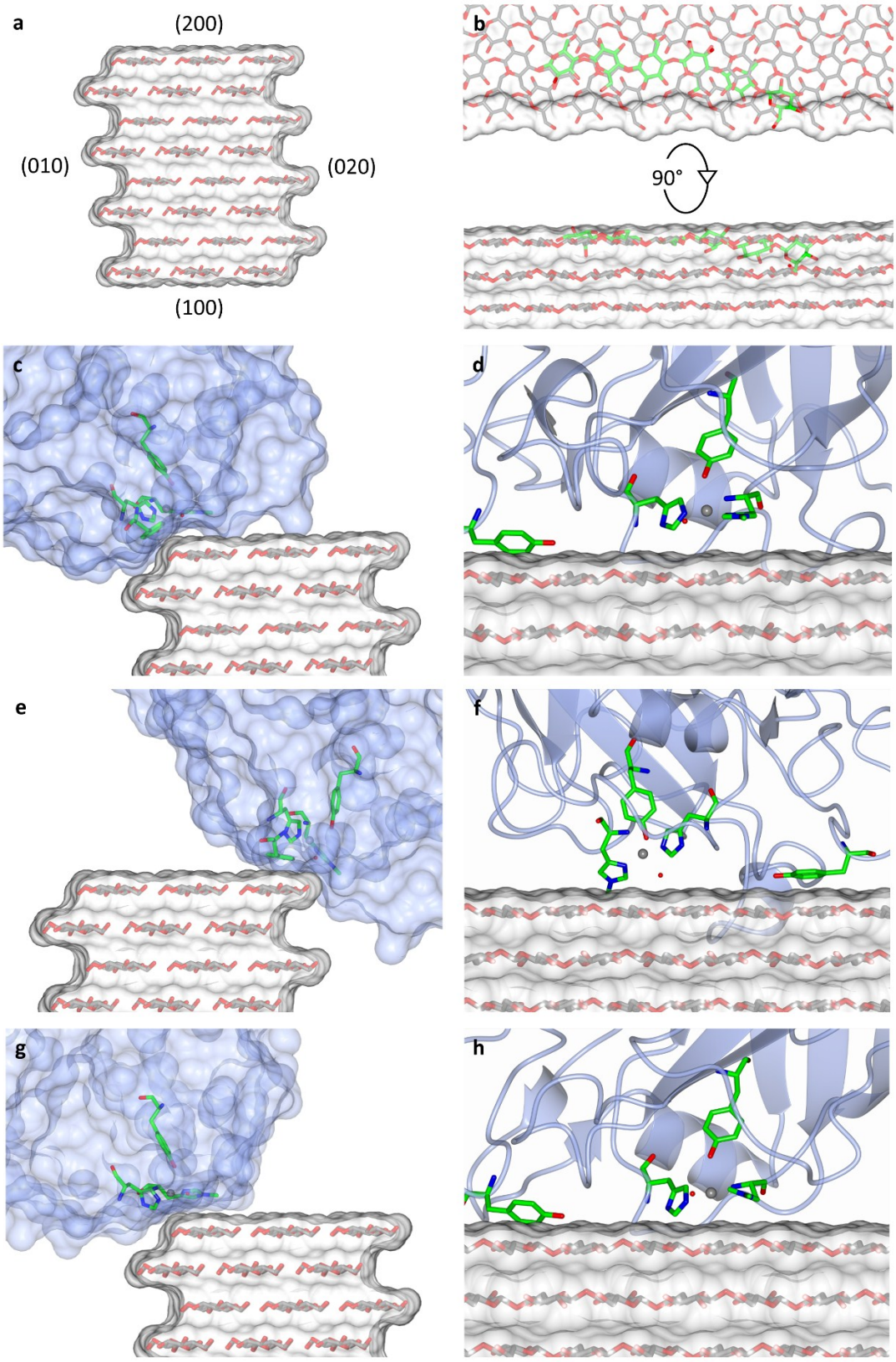

Fig. S11 (a) Model of celery cellulose fibrils viewed from the non-reducing end with annotation of crystal faces. (b) Overlap of cellohexaose from 5ACI with cellulose fibrils viewed from the top and the side. (c, d) Model of *Ls*AA9A bound to the (200)-(010) edge. (d, f) Model of *Ls*AA9A bound to the (200)-(020) edge. (g, h) Model of *Ta*AA9A bound to the (200)-(010) edge. Water molecule in the equatorial position showed as a red sphere.

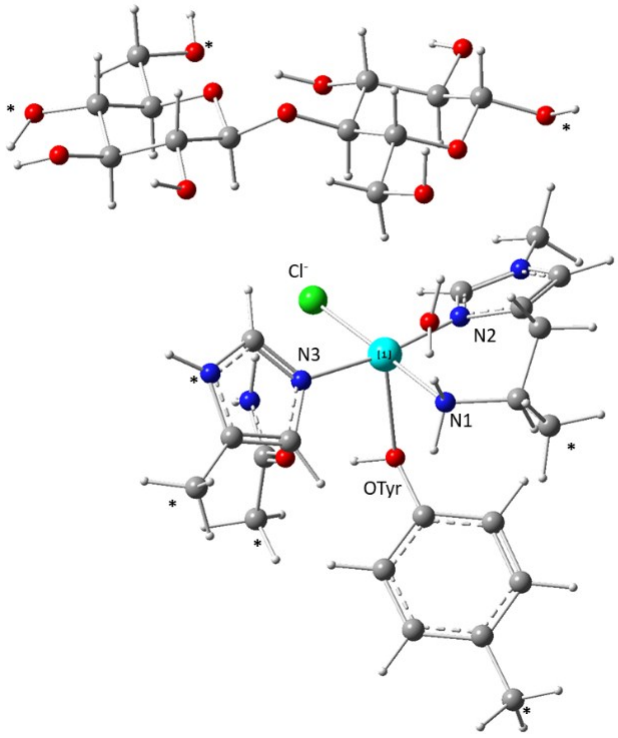

Fig. S12 Starting structure for geometry optimization of the *Ls*AA9A active site; Cu is represented as light blue sphere. Asterisks denote frozen atoms during optimizations.

Table S1 Calculated Spin Hamiltonian parameters for *g* and A^{Cu} tensors, and relative eigenvectors matrix (written as column vectors).

	g_1	g_2	g_3	A_1 (MHz)	A_2 (MHz)	A_3 (MHz)
	2.056	2.080	2.223	7	65	-572
eigenvectors						
X	-0.9909	0.0032	-0.1348	-0.0395	-0.9903	0.1335
Y	-0.0002	0.9997	0.0253	0.9985	-0.0441	-0.0317
Z	0.1348	0.0251	-0.9906	0.0372	-01321	0.9905
Label[1]	g_x	g_y	g_z	A_y	A_x	A_z

[1]-Labels are assigned according to the eigenvectors orientation with respect to the molecular reference frame

Table S2 Selected distances and angles for optimized structures of the *Ls*AA9A active site. For comparison, distances and angles measured from the crystal structure (5ACF) are also included. Atom numbers refer to the numbers shown in the figure above.

	Cu-N1 (Å)	Cu-N2 (Å)	Cu-N3 (Å)	Cu-OTyr (Å)	Cu-X$^-$ (Å)	N1-Cu-N2	N1-Cu-N3	N2-Cu-N3	N1-Cu-X-	N2-Cu-X-	N3-Cu-X-
DFT model	2.12	2.01	2.03	2.42	2.37	90.3°	88.6°	164.3°	176.1°	91.3°	88.9°
Crystal Structure (5ACF)	2.16	1.88	2.06	2.47	2.34	90.3°	90.3°	169.8°	175.1°	93.1°	85.8°

Appendix. List of the atomic coordinates for the geometry optimized active site model used in DFT calculations.

N	0.000000000	-2.123065000	0.000000000
C	1.257170000	-2.907897000	-0.131053000
C	1.029144000	-4.411927000	0.053697000
C	2.292904000	-2.343320000	0.851844000
C	2.831885000	-1.031228000	0.390631000
C	4.133417000	-0.620728000	0.255663000
N	2.008128000	0.011499000	0.000000000
C	2.799270000	1.021684000	-0.345634000
N	4.094471000	0.678039000	-0.208314000
C	5.243310000	1.554372000	-0.386822000
C	-5.489765000	-1.194731000	0.502776000
C	-4.130071000	-0.614122000	0.678479000
C	-2.948705000	-0.848983000	0.017665000
N	-3.823246000	0.346788000	1.626992000
C	-2.510867000	0.662766000	1.518053000
N	-1.953678000	-0.050646000	0.549744000
C	-2.055356000	2.996757000	-4.839422000
C	-1.612167000	2.908546000	-3.402259000

N	-0.838174000	3.866210000	-2.879093000
O	-1.958990000	1.911580000	-2.743592000
C	-1.271846000	-4.825773000	-5.572928000
C	-1.069807000	-3.590463000	-4.711468000
C	0.204919000	-3.237168000	-4.232743000
C	-2.131636000	-2.726645000	-4.389402000
C	0.413487000	-2.080013000	-3.476664000
C	-1.942866000	-1.568583000	-3.622246000
C	-0.660809000	-1.236700000	-3.156759000
O	-0.412150000	-0.137147000	-2.375827000
Cu	0.000000000	0.000000000	0.000000000
Cl	-0.065257000	2.368736000	0.148234000
O	5.154842000	0.779113000	2.763617000
C	4.110767000	1.479649000	3.368993000
C	3.884351000	2.880757000	2.756744000
O	5.057737000	3.648891000	2.862591000
C	2.703007000	3.564411000	3.483193000
O	2.435921000	4.826942000	2.874563000
C	1.483582000	2.639664000	3.454653000
O	0.469284000	3.082024000	4.347948000
C	1.811244000	1.204291000	3.889958000
O	2.933565000	0.713715000	3.188497000
C	0.629794000	0.288639000	3.606286000
O	0.837487000	-1.053026000	4.034967000
C	-0.410171000	4.033227000	3.883677000
C	-1.755686000	3.818155000	4.552845000
O	-2.284614000	2.570465000	4.145287000
C	-2.695121000	4.953958000	4.186593000
O	-3.884158000	4.732163000	4.904803000
C	-2.083282000	6.318547000	4.493121000
O	-2.997840000	7.290265000	4.015949000
C	-0.707186000	6.414466000	3.817767000
O	0.090543000	5.316309000	4.253688000
C	0.056552000	7.678197000	4.153391000
O	1.243229000	7.678310000	3.389413000
O	-0.914397000	-2.666517000	2.654664000
H	-3.132027000	2.781178000	-4.882781000
H	-1.851269000	3.964813000	-5.319401000
H	-0.545323000	4.677059000	-3.409248000
H	-0.507353000	3.734374000	-1.922163000
H	-0.455890000	-2.371898000	0.895776000
H	1.628878000	-2.739163000	-1.150691000
H	1.830665000	-2.236472000	1.849634000
H	3.128015000	-3.050333000	0.959167000
H	5.068463000	-1.127004000	0.474942000
H	2.453616000	1.992993000	-0.684361000
H	4.922330000	2.467734000	-0.903456000
H	5.662385000	1.813613000	0.595361000
H	6.006992000	1.048919000	-0.994073000
H	-5.833913000	-1.703090000	1.418704000
H	-5.479354000	-1.931616000	-0.311710000
H	-2.767474000	-1.519186000	-0.816956000
H	-4.470146000	0.761243000	2.288511000

H	-2.021352000	1.407586000	2.139124000
H	-2.299998000	-5.209990000	-5.491572000
H	-0.578605000	-5.631715000	-5.286905000
H	1.062031000	-3.875875000	-4.466192000
H	-3.139587000	-2.960928000	-4.744724000
H	1.414453000	-1.803716000	-3.139868000
H	-2.782183000	-0.908691000	-3.390347000
H	4.303107000	1.603957000	4.458687000
H	3.590414000	2.729649000	1.699831000
H	4.795469000	4.565046000	2.681899000
H	3.003487000	3.702712000	4.541474000
H	1.816331000	5.329922000	3.436157000
H	1.098604000	2.622411000	2.421308000
H	2.015918000	1.213538000	4.982007000
H	-0.278862000	0.728835000	4.048136000
H	0.490651000	0.240531000	2.518090000
H	0.872758000	-1.077730000	5.002385000
H	-0.517256000	3.978532000	2.781258000
H	-1.584127000	3.837118000	5.646066000
H	-3.195149000	2.540434000	4.476730000
H	-2.879505000	4.910436000	3.092757000
H	-4.491303000	5.455664000	4.688969000
H	-1.949078000	6.394827000	5.588368000
H	-2.921099000	8.091947000	4.548394000
H	-0.844137000	6.371449000	2.719143000
H	-0.589210000	8.547027000	3.919507000
H	0.261430000	7.684083000	5.241783000
H	1.829096000	8.373418000	3.715122000
H	-0.304132000	-2.141618000	3.220433000
H	-0.824779000	-3.574302000	2.974860000
H	5.189078000	-0.094141000	3.178742000
H	0.684137000	-4.630754000	1.076999000
H	0.270625000	-4.782629000	-0.653624000
H	1.963131000	-4.966335000	-0.123743000
H	-0.635182000	-2.393222000	-0.752026000
H	-6.232346000	-0.419349000	0.251441000
H	-1.088509000	-4.598243000	-6.637370000
H	-1.083193000	0.596149000	-2.510971000
H	-1.538366000	2.201917000	-5.399697000

References

1. K. E. H. Frandsen, T. J. Simmons, P. Dupree, J.-C. N. Poulsen, G. R. Hemsworth, L. Ciano, E. M. Johnston, M. Tovborg, K. S. Johansen, P. von Freiesleben, L. Marmuse, S. Fort, S. Cottaz, H. Driguez, B. Henrissat, N. Lenfant, F. Tuna, A. Baldansuren, G. J. Davies, L. Lo Leggio and P. H. Walton, *Nature Chemical Biology*, 2016, **12**, 298.
2. *Novozymes A/S Pat.,* Patent WO2014066141 A2, 2014.
3. P. V. Harris, D. Welner, K. C. McFarland, E. Re, J.-C. Navarro Poulsen, K. Brown, R. Salbo, H. Ding, E. Vlasenko, S. Merino, F. Xu, J. Cherry, S. Larsen and L. Lo Leggio, *Biochemistry*, 2010, **49**, 3305-3316.

4. A. Šturcová, I. His, D. C. Apperley, J. Sugiyama and M. C. Jarvis, *Biomacromolecules*, 2004, **5**, 1333-1339.
5. L. H. Thomas, V. T. Forsyth, A. Šturcová, C. J. Kennedy, R. P. May, C. M. Altaner, D. C. Apperley, T. J. Wess and M. C. Jarvis, *Plant Physiology*, 2013, **161**, 465-476.
6. G. Vaaje-Kolstad, B. Westereng, S. J. Horn, Z. Liu, H. Zhai, M. Sørlie and V. G. H. Eijsink, *Science*, 2010, **330**, 219-222.
7. S. Stoll and A. Schweiger, *Journal of Magnetic Resonance*, 2006, **178**, 42-55.
8. Gaussian 09 Revision D.01, M. J. T. Frisch, G. W.; Schlegel, H. B.; Scuseria, G. E.; Robb, M. A.; Cheeseman, J. R.; Scalmani, G.; Barone, V.; Mennucci, B.; Petersson, G. A.; Nakatsuji, H.; Caricato, M.; Li, X.; Hratchian, H. P.; Izmaylov, A. F.; Bloino, J.; Zheng, G.; Sonnenberg, J. L.; Hada, M.; Ehara, M.; Toyota, K.; Fukuda, R.; Hasegawa, J.; Ishida, M.; Nakajima, T.; Honda, Y.; Kitao, O.; Nakai, H.; Vreven, T.; Montgomery, J. A., Jr.; Peralta, J. E.; Ogliaro, F.; Bearpark, M.; Heyd, J. J.; Brothers, E.; Kudin, K. N.; Staroverov, V. N.; Kobayashi, R.; Normand, J.; Raghavachari, K.; Rendell, A.; Burant, J. C.; Iyengar, S. S.; Tomasi, J.; Cossi, M.; Rega, N.; Millam, J. M.; Klene, M.; Knox, J. E.; Cross, J. B.; Bakken, V.; Adamo, C.; Jaramillo, J.; Gomperts, R.; Stratmann, R. E.; Yazyev, O.; Austin, A. J.; Cammi, R.; Pomelli, C.; Ochterski, J. W.; Martin, R. L.; Morokuma, K.; Zakrzewski, V. G.; Voth, G. A.; Salvador, P.; Dannenberg, J. J.; Dapprich, S.; Daniels, A. D.; Farkas, Ö.; Foresman, J. B.; Ortiz, J. V.; Cioslowski, J.; Fox, D. J., Gaussian, Inc., Wallingford, CT, 2016.
9. A. Schäfer, C. Huber and R. Ahlrichs, 1994, **100**, 5829-5835.
10. F. Weigend and R. Ahlrichs, *Physical Chemistry Chemical Physics*, 2005, **7**, 3297-3305.
11. S. Grimme, J. Antony, S. Ehrlich and H. Krieg, 2010, **132**, 154104.
12. F. Neese, 2018, **8**, e1327.
13. F. Neese, *Inorganica Chimica Acta*, 2002, **337**, 181-192.
14. W. Kutzelnigg, U. Fleischer and M. Schindler, Berlin, Heidelberg, 1991.